Hindawi Publishing Corporation
Advances in OptoElectronics
Volume 2016, Article ID 7182303, 7 pages
http://dx.doi.org/10.1155/2016/7182303

Research Article

Polarization Sensitive Reflection and Dielectric Spectra in GaSe Thin Films

Hazem K. Khanfar[1] and Atef A. Qasrawi[2,3]

[1]*Department of Telecommunication Engineering, Arab-American University, Jenin, State of Palestine*
[2]*Department of Physics, Arab-American University, Jenin, West Bank, State of Palestine*
[3]*Group of Physics, Faculty of Engineering, Atilim University, 06836 Ankara, Turkey*

Correspondence should be addressed to Atef A. Qasrawi; atef.qasrawi@atilim.edu.tr

Received 10 March 2016; Revised 16 June 2016; Accepted 5 July 2016

Academic Editor: Armin Gerhard Aberle

The light polarization effects on the optical reflective and dielectric spectra of GaSe thin films are studied in the incident light wavelength range of 200–1100 nm. In this range of measurement, the angle of incidence (θ_i) of light was varied between 30° and 80°. In addition, at θ_i of 30° the light polarizing angle (δ) was altered in the range of 0–90°. Regardless of the value of λ, for all $\theta_i > 65°$, the total reflectance sharply decreased with increasing θ_i. In addition, when θ_i is fixed at 30° and δ was varied, the amplitudes ratio of the polarized waves exhibits a resonance-antiresonance phenomenon at a wavelength that coincides with the film's thickness (800 nm). This behavior was assigned to the coupled interference between incident and reflected waves and to the strong absorption effects. Two main resonance peaks are observed as response to *s*-polarized and normal incident beam: one is at ~540 (556 nm) and the other at ~420 THz (714 nm). The dielectric constant of the GaSe films exhibits anisotropic characteristics that nominate it for use as multipurpose optoelectronic devices.

1. Introduction

Optical communications technologies, which include visible light communication (VLC), free space optical communication (FSO), Li-Fi, and infrared data transformers, are one important part of our daily life needs. Data transformations using the VLC technology, which get use of light in the frequency range of 400–800 THz, are very new and attract the focus of much research and development centers. In a trail to use VLC system for data transformation, in the year 2010, a 500 Mbit/s data transformation rate over few meters' distance was successfully actualized using white LED (light emitting diode) as encoding light source [1, 2]. In the following year a live high-definition video was transmitted from a standard LED lamp by TED Global. However, long distance (~1.5 km) data transformation is still actualized at low rates.

The VLC technology translates the optical data to electrical signal via photosensitive substrates. In this operation, the time it takes to switch on and off electric current determines the rate at which signals can be processed [3]. In addition, the control of electric current on a subpicosecond timescale in semiconductors is now possible through the optical injection of currents by the help of interfering photoexcitation pathways [3, 4] or photoconductive switching of terahertz transients. The reversibility of the AC conductivity in silica is reported to be enhanced by 18 times in one femtosecond [5] by the incident electric field (light wave) polarization. In the scope of these requirements and developments there is a need to find new types of optical substrates that allow electric field interference in the visible region to fit with the VLC technology needs. One of these substrates is the well-known photovoltaic copper indium gallium selenide photocell [6]. A TD06006M-01278 C05-33 copper indium gallium selenide photocell of 80 × 45 mm dimensions was used to analyze Li-Fi performances under different lighting conditions. This cell has revealed a band width up to 4.2 MHz at 80 lx DC. On the other hand, when the gallium selenide optoelectronic device is excited with a 405 nm laser at a power of 0.5 mW/mm^2 it reflected a dark to light current ratio of the order 10^3 [7]. The photoresponsivity and quantum efficiency of this device

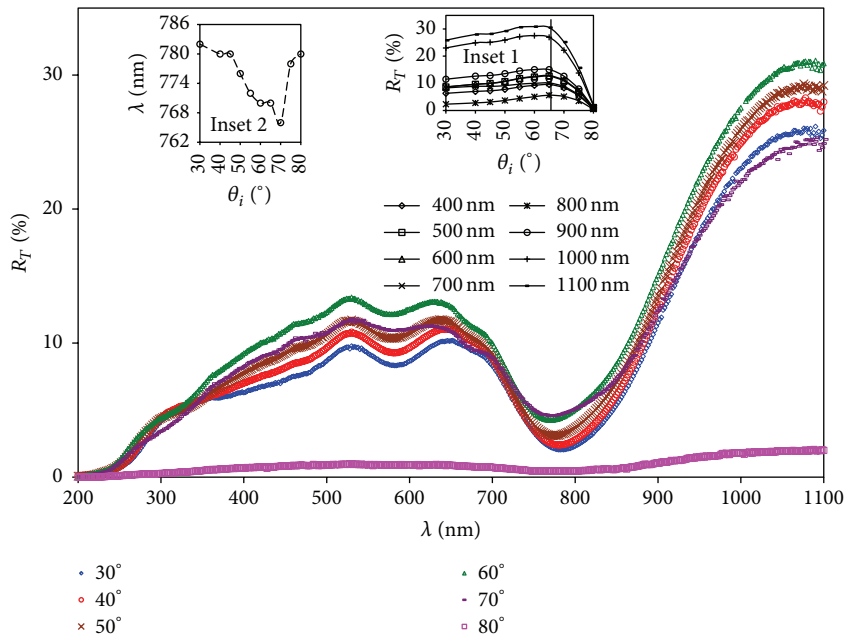

FIGURE 1: The total unpolarized reflection (R_T) spectra for GaSe films. Inset 1 and inset 2 display $R_T - \theta_i$ dependence and the absolute minimum position as a function of θ_i.

are reported as 17 mA/W and as 5.2%, respectively. These parameters are promising as it indicates the applicability of GaSe in photosensing technology. The reflectivity from the GaSe film surface is less than 35%. It significantly decreases in the wavelength region of 600–850 nm. As a result, owing to the photon-plasmon coupling, the dielectric constant exhibits minima at 850 nm. Our previous studies on plasmon-electron interactions at the surface of GaSe indicated that the GaSe could exhibit an ultrafast photoconduction response. The optical conduction parameter appears to be promising for using the GaSe in the technology of midinfrared plasmonic nanoantennas [8]. Thus, here in this work, we will discuss the effect of angle of incidence of light and angle of polarization at a particular angle of incidence on the optical dielectric spectra of GaSe thin film prior to use in VLC technology.

2. Experimental Details

GaSe thin films were deposited onto chemically cleaned glass substrates via the physical vapor deposition technique using NORM 600 thin film evaporator under a pressure of 10^{-6} mbar. The source material was Ga_2Se_3 (Alfa Aesar) single crystals. The obtained films were found to exhibit the polycrystalline nature of structure as tested by the X-ray diffraction technique. The three observed peaks which appeared at interplaner spacing values of 3.977, 2.515, and 1.687 Å indicated a polyphase of hexagonal GaSe crystal structure that is oriented in (004), (104), and (111) directions, respectively. The optical measurements of the films were carried out using Thermo-Scientific Evolution 300 spectrophotometer. This device is equipped with VEEMAX variable angle reflectometer and a variable angle polarizer.

3. Results and Discussion

Some of the total unpolarized light reflection (R_T) spectra (light is directed from the source to the sample through optical assembly not containing polarizer accessory) of the GaSe thin films which were recorded in the incident wavelength range of 200–1100 nm at various angles of incidence in the range of 30–80° are displayed in Figure 1. As can be seen, at a particular angle of incidence (θ_i), the figure reflects two positions of reflection peaks located at 530 and 640 nm. It is also observed that, regardless of the angle of incidence, R_T spectra exhibit a sharp decrease in the wavelength range of 640–780 nm. In the near infrared range (800–1000 nm) the reflectance increases with increasing λ. For higher λ values, R_T tends to remain constant. In addition, a remarkable shift in the values of absolute minima which are associated with increasing angle of incidence can be observed from inset 2 of Figure 1. The minimum reflectivity which is observed at 780 nm shifts to 766 nm as θ_i reaches 70°. Moreover, for larger values of θ_i, R_T reincreases. On the other hand, inset 1 of Figure 1 displays the variation of total reflectance as a function of angle of incidence being presented at different wavelength values. For all curves which represent different photon energies, the reflectivity increases with increasing angle of incidence till a critical angle (θ_c) of 65° is reached. For all $\theta_i \succ \theta_c$, R_T sharply decreases, reaching zero value near 80°.

The reflection peaks which appeared at 530 (2.34 eV) and 640 nm (1.94 eV) can be ascribed to the direct allowed electronic transitions from the valence to the conduction band of δ-GaSe and ε-polytypes. The GaSe polytypes are described in terms of the stacking of the hexagonal layers of D_{3h} symmetry. In accordance with this symmetry four

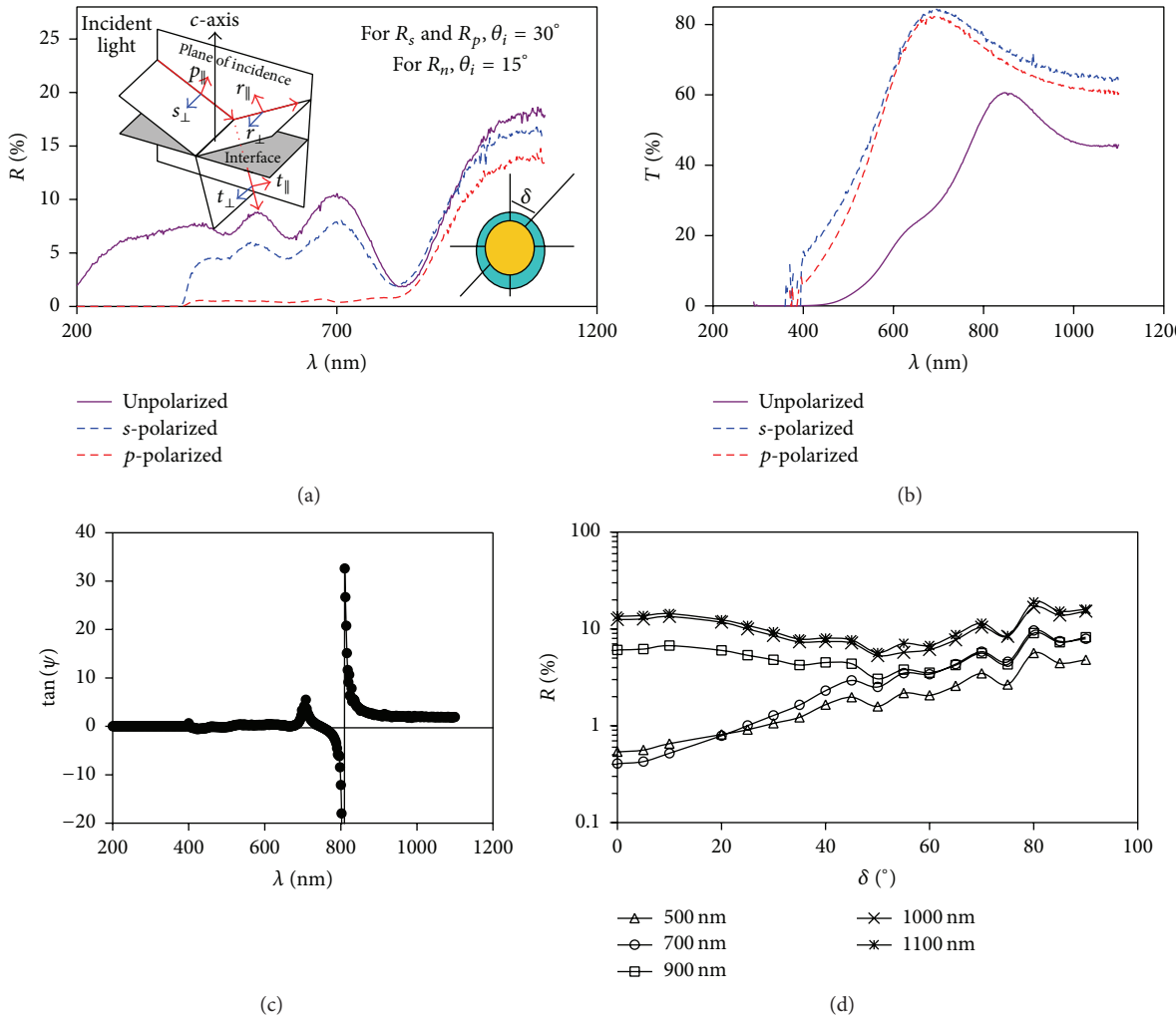

FIGURE 2: ((a) and (b)) The normal (unpolarized), parallel ($R_p = |r_\parallel|^2$, $T_p = |t_\parallel|^2$), and perpendicular ($R_s = |r_\perp|^2$, $T_s = |t_\perp|^2$) polarized reflection and transmission spectra for GaSe films, respectively. (c) $R - \delta$ variation at a particular λ. (d) $\tan\psi - \lambda$ dependence. The inset of (a) shows the geometrical design of the polarization vectors.

types can exist. While δ-GaSe reveal an energy band gap of 2.01 eV, ε-GaSe reveal an energy band gap of 2.34 eV [9, 10]. On the other hand, while the minimum which appeared in the total reflectance at 780 nm (1.59 eV) may be assigned to the indirect allowed electronic transitions in one of the polytypes, the continuous increase in R values with decreasing incident photon energy is attributed to the enhanced interband transitions at this excitation level.

As the measured R_T is equal to $(R_s+R_p)/2$ [11] with R_s and R_p being the components of the incident light which is polarized with its electric field being perpendicular (transverse electric polarization (TE)) and parallel (transverse magnetic polarization (TM)) to the plane of incidence (the geometry of polarization is shown in the inset of Figure 2(a), resp.), the effect of polarization angle (δ) on the total reflectivity is studied and presented in Figure 2(b). For this purpose, θ_i was fixed at 30° and δ was varied in the range of 0° to 90°. As may be seen from Figure 2(b), the reflection coefficient of the GaSe films basically depends on the values of δ and λ. Namely, for all λ values in the visible region, R values continuously increase with increasing δ. In the IR region, R values show a decreasing trend with increasing δ up to 50° where it starts increasing again. From the photon energy point of view, such behavior may be assigned to strong absorbability of the GaSe films in the visible region. The GaSe films exhibit strong absorption in the region of 400–700 nm (not shown). From polarization angle points of view, the parameters which are measured represent the changes in the amplitude and phase of the incident light. Those are usually presented by the angles ψ and Δ, respectively. These two angles relate to the complex reflectance ratio (ρ) of s and p polarization directions in which $\rho = r_p/r_s = \tan(\psi)\exp(i\Delta)$. The focus on this ratio arises for its physical meaning which gives all relevant information about the polarization state of the light at a given wavelength. It indicates the phase difference between the electric field components of the reflected waves. The square of ratio reduces the phase effect that arises from the GaSe surface and provides information about the wave

amplitudes only (reflected intensities). Since the amplitude increases exhibiting maxima when two waves which are in phase interfere or it decreases when waves exhibiting phase difference interfere, the (ρ) ratio maxima and minima are governed by the interferences rather than the reflectances themselves.

The complex reflectance ratio itself depends on complex dielectric constant, the film thickness, the angle of incidence, and the wavelength [11, 12]. Evaluating $\rho^2 = R_p/R_s = \tan^2(\psi)$ reveals the relation between $\tan(\psi)$ and the incident photon wavelength. $\tan(\psi) - \lambda$ variation which is presented in Figure 2(c) shows that the amplitude ratio upon reflection exhibits ~6-time magnification at 708 nm followed by a resonance (at 808 nm) antiresonance (at 810 nm) mechanism. This point coincides with the film thickness, which is measured and found to be 800 nm. In this process, the light waves reflected by the upper and lower boundaries of a thin film interfere with one another to form a new wave. When the thickness of the film is quarter-multiple of the wavelength of the light, the reflected waves from the top and bottom of the GaSe and glass surfaces, respectively, interfere to "destroy" each other. Since the wave cannot be reflected, it is completely transmitted instead. On the other hand, when the thickness is half-multiple of the wavelength within the GaSe film, both reflections from bottom and top of the film interfere to build each other up, increasing the reflected wave and reducing the transmission. This causes certain wavelengths to be intensified while others are attenuated [11, 12]. Another reason for the resonance case which appears in Figure 2(c) may also be obtained by considering that the amplitude of the polarization vector ($\vec{P}$) depends on the incident wave angular frequency (ω) and on the effective resonance angular frequency of the bound electrons (w_o) through the relation $P \propto (w_o^2 - w^2 - iw\gamma)^{-1}\vec{E}$ with $\vec{E}$ being the incident electric field vector and γ being defined as the frictional damping coefficient that is proportional to the velocity of electrons. In accordance with this equation, the optical resonance happens to light frequencies in the neighborhood of the resonance frequency (w_o). It takes place due to the large change in the index of refraction of the medium and due to the strong absorption of light near w_o [12]. In accordance with this approach, a large change in the refractive index value happens when the light reaches the end of the GaSe film where it penetrates to the glass which has lower refractive index leading to a change in the wave velocity.

Additionally, the reflectance spectra which are presented in Figure 2(a) compare the normal reflection coefficient (normal reflection is measured at angle of 15° without polarizer) of the GaSe films to those which arise from the light polarizations in s and p directions (light is incident at angle of 30° before arrival at the polarizer surface). As may be seen from this figure, the normal incidence (R_n) of light reveals an increasing R_n value, followed by peaking behavior that appears at the same positions which are observed at all angles of incidence. The same peaks are also observed for s-polarized light. The reflectivity at normal incidence is higher than those of s-polarized till the wavelength of incident light exceeds 780 nm. For all the remaining IR range there is no significant difference between s, p, and normal reflectivity. However, a clear shift in the value of the absolute minima of reflectance when light is incident with particular direction is readable from the figure. The difference between s and p reflectivity values from that of normal incidence indicates information about the anisotropic nature of the layered type GaSe films. However, the direct method to determine the anisotropic property of the GaSe layer is to measure the transmittance spectra at normal incidence with s and p polarization directions. The measured data of transmittance for light being incident at $\theta_i < 5°$ (normal incidence) are displayed in Figure 2(d). The normal transmittance which appears in Figure 2(d) means being measured without polarization. T_s and T_p polarized mean those which relate to s and p polarization directions with light being incident at $\theta_i < 5°$ (regarded as normal incidence). As the figure displays all incident light of wavelength less than 600 nm and greater than 700 nm, T_p and T_s spectra do not overlap confirming the anisotropic nature of GaSe material as observed from reflectivity measurements. The reason for the high values of the nonpolarized T and R compared to T_p and T_s and R_p and R_s, respectively, is ascribed to the electric field components of incident light vector ($E = E_s + E_p$). For example, $R_s = |E_s|^2/|E|^2 = |\sin(\theta_1 - \theta_2)/\sin(\theta_1 + \theta_2)|$ and $R_p = |E_p|^2/|E|^2 = |\tan(\theta_1 - \theta_2)/\tan(\theta_1 + \theta_2)|$, with θ_1 and θ_2 being the angles of incidence and refracted light, respectively ($n_1 \sin\theta_1 = n_2 \sin\theta_2$, n_1: air, n_2: GaSe). In accordance with these equations, R or T ($T = 1 - R - A$, A: absorbance) exhibit higher or lower values depending on the value of refractive index of the GaSe at any particular wavelength in addition to the absorbed amount of incident light. In addition, when light makes multiple reflections between two parallel surfaces (GaSe and glass), the multiple beams of light interfere with one another, and the surfaces act as a Fabry-Perot interferometer. This effect is responsible for the ripples which appear in R and T spectra.

The data of R_n, R_s, and R_p are used to determine ε_n, ε_s, and ε_p which are the dielectric constants due to the normal, s-, and p-polarized light beams, respectively, through Fresnel's equations by the substituting of the value of θ_i as 30° and using the measured data for R_s and R_p, the relative dielectric spectra were determined and displayed in Figure 3(a). For R_n the calculations were done for normal incidence case of Fresnel equations [13, 14]. In general, the effective dielectric constants (ε represents either ε_n, ε_s, or ε_p) $\varepsilon = \varepsilon_r + i\varepsilon_{\text{im}}$, where ε_r and ε_{im} are the real and imaginary parts, respectively. They are related to the effective dielectric constant through the relations $\varepsilon_r^2 = \varepsilon - k^2$ and $\varepsilon_{\text{im}} = 2\sqrt{\varepsilon}\kappa$. Here, $\kappa = \alpha\lambda/4\pi$ is the extinction coefficient, which directly depends on the absorption coefficient (α) [13–15]. The real part of dielectric constant spectra is displayed in Figure 3(b). On the other hand, the dielectric quality factor Q which is defined as the inverse of the loss tangent ($\tan(\xi) = \varepsilon_{\text{im}}/\varepsilon_r$) is also calculated and displayed in Figure 3(c).

The figure displays interesting characteristics of the dielectric constant of the GaSe films. Namely, the dielectric spectra are influenced by the incident field polarization direction. When the light was incident normal to the film

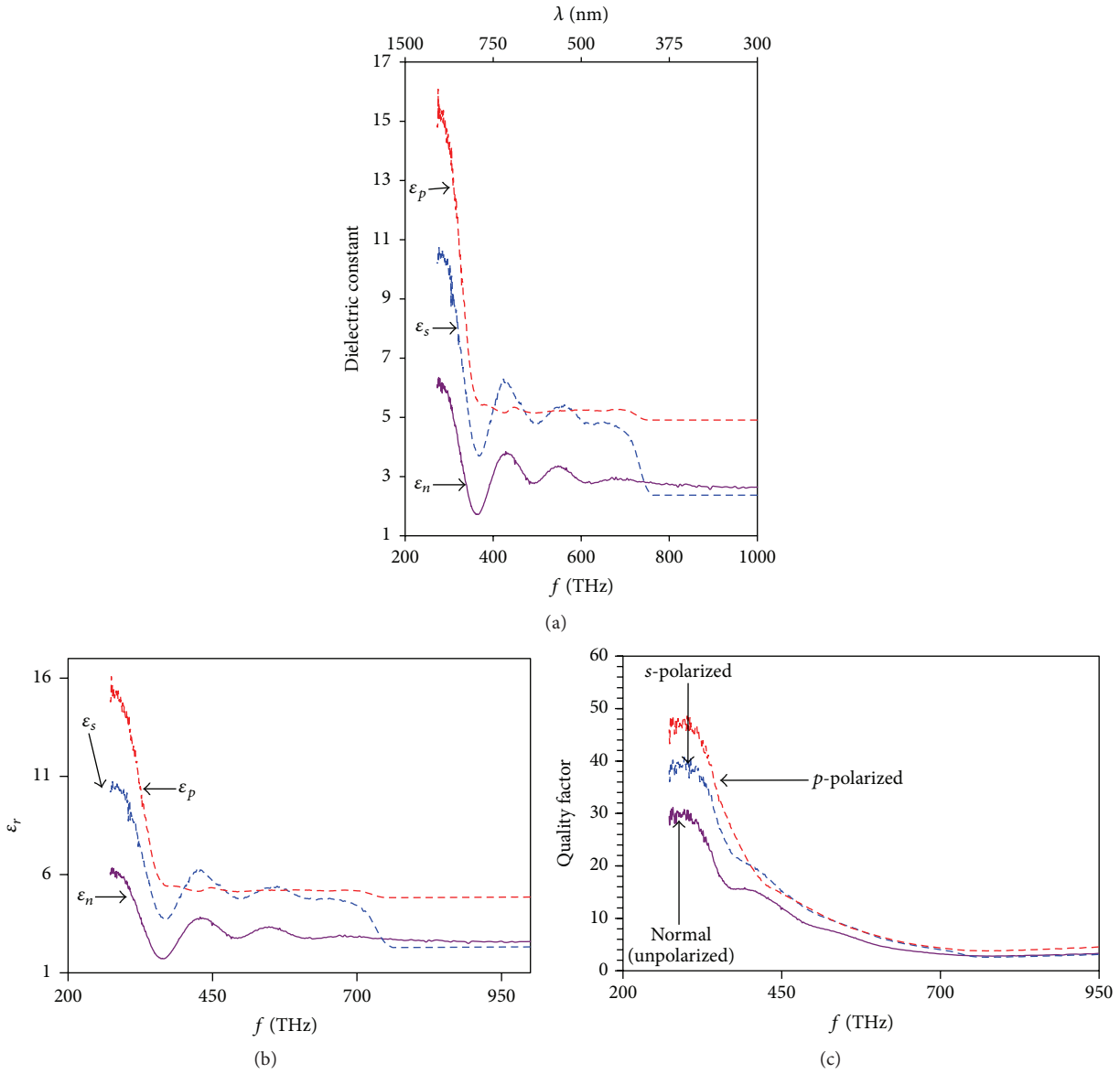

FIGURE 3: (a) The effective dielectric spectra for the normal p- and s-polarized light. (b) The real dielectric constant spectra and (c) the quality factor spectra.

surface with an unpolarized beam of light and when the light was polarized parallel to the plane of incidence, both of the effective ε_n and ε_s values exhibited one minor and one major resonance peak at 545 and 423 THz for ε_s spectra and at 540 and 420 THz for ε_n spectra, respectively. For lower applied frequencies all the dielectric constant parts sharply increased with decreasing frequency. The evaluated $(\varepsilon_p/\varepsilon_s)$ ratio in the frequency range of 360–270 THz is found to be ~1.45 and that of $\varepsilon_p/\varepsilon_n$ is ~2.5. Both ratios indicate the dominant anisotropic dielectric properties of GaSe thin films. The evaluated real dielectric constant and quality factor of these spectra which are displayed in Figures 3(b) and 3(c), respectively, show the same positions of resonance with a quality factor of ~30–50 in the low terahertz frequency region.

The differences between the values of ε_s and ε_p could be assigned to the optical anisotropy [16, 17] in GaSe. Recent reports on this material have shown that the energy positions of the absorption edges vary with the orientation of plane-polarized light relative to the crystallographic c-axis. The absolute values of the optical absorption coefficient for the GaSe for $\vec{E}$ parallel to c (c-axis of GaSe is perpendicular to the film's surface as shown in the inset of Figure 2(a)) and $\vec{E}$ perpendicular to c light orientations are reported to be ~10^4-10^5 and 10^3 cm^{-1}, respectively. Consistent with our observation, the optical anisotropy presented by the dielectric dispersion of the GaSe was also theoretically estimated through the ab initio calculations of the optical constants [18] of GaSe layered crystals. The dielectric functions, refractive indices, and

extinction coefficients of GaSe layered crystals which were theoretically calculated using the density functional theory have shown that the optical functions can be characterized by the most pronounced polarization anisotropy in the range of photon energies of ~4–7 eV. The results obtained for the dielectric anisotropy of GaSe crystal are close in numerical values and on variation trends for the GaSe films reported here.

Recalling that the dielectric constant is a measure of the ability to reduce any electric field setup in the GaSe films, then the values of the effective dielectric constant indicate that GaSe films behave as semiconductor which permits electric field setup easily at the films surface especially near IR frequencies. However, such behavior is hardly possible when incident light is unpolarized. In other words, the optical conductivity ($\sigma(w)$), which is obtainable from the relation $\varepsilon = \varepsilon_{\text{core}} + (4\pi i/w)\sigma(w) = \varepsilon_r + i\varepsilon_{\text{im}}$ [14, 15] at particular angular frequency $w = 2\pi c/\lambda$, is directly proportional to the imaginary part of the dielectric constant. Thus, the spectra of $\sigma(w)$ provide information about the regions of poor and high conductivity values. While it makes slight difference between the values of the parallel and perpendicular incident electric fields, the unpolarized field reveals higher optical conductivity.

An anisotropic dielectric effect of the light being polarized perpendicularly to SiO_2 surface was observed by Schiffrin et al. [5]. *s* polarization was made to drift the generated carriers toward two Au electrodes which are designed to catch the electrical signal that arises from optical excitations. Schiffrin et al. were able to demonstrate that perpendicularly polarized optical fields are capable of transforming the dielectric material into a state of highly increased polarizability, which allow the optical currents to flow and result in macroscopic charge separation that is detectable in an external circuit.

The mechanism of the dielectric and reflection spectra which are presented in Figures 1, 2, and 3 can be explained by focusing on the dynamics of electromagnetic radiation. The electromagnetic wave which is incident on the film surface induces small oscillations of polarization in the individual atoms, causing each atom to emit a secondary wave in all directions. Emitted electromagnetic waves add up to give the total specular reflection and refraction in accordance with the Huygens-Fresnel principle. As the GaSe films are nonmetals, $\vec{E}$ component of the light acts on the charge carriers of the film surface and on the bulk during the transmission process. The moving charge carriers generate a new electric field and become radiator. As a result, the refraction of light in the film can be regarded as the combination of the forward radiation of the charge carriers and the incident light and the backward radiation is the one which is accepted as reflected from the surface of the film.

In the reflection resonance peak regime, the field undergoes multiple reflections throughout the structure which result in the slowing down and confinement of light at this regime and which lead to a strong nonlinear interaction [19, 20]. Thus, the resonance which appears at ~540 and 420 THz takes place whenever the incident and radiated fields couple and oscillate at the same frequency. On the other hand, whenever a phase change in the incident and radiated fields exists due to changes in the angle of incidence and/or due to the increase in the light energy, *R* values are reduced and/or shifted as shown in the insets of Figure 1 [19, 20].

4. Conclusions

In this work, the optical dynamics on the GaSe thin film surface are studied and analyzed. The material is observed to exhibit very interesting characteristics that nominate it as an attractive optical element which can be used to cause resonance of light pulses of 540 and 420 THz frequencies if the incident light is polarized perpendicular to the plane of incidence. These two pulses are promising for use in optical communications and suggest that the GaSe films could be promising material for use in wireless communications.

Competing Interests

The authors declare that there are no competing interests regarding the publication of this paper.

Acknowledgments

This research was funded by the AAUJ research deanship through the first cycle II of 2014/2015. Therefore, the authors would like to acknowledge and submit thanks to the university president, the dean of scientific research, and all the scientific research council members at the AAUJ.

References

[1] Siemens, "500 Megabits/Second with White LED Light," 2010.

[2] W. Zhang and M. Kavehrad, "A 2-D indoor localization system based on visible light LED," in *Proceedings of the IEEE Photonics Society Summer Topical Meeting Series (PSST '12)*, pp. 80–81, Seattle, Wash, USA, July 2012.

[3] L. Prechtel, L. Song, S. Manus, D. Schuh, W. Wegscheider, and A. W. Holleitner, "Time-resolved picosecond photocurrents in contacted carbon nanotubes," *Nano Letters*, vol. 11, no. 1, pp. 269–272, 2011.

[4] I. Franco, M. Shapiro, and P. Brumer, "Robust ultrafast currents in molecular wires through stark shifts," *Physical Review Letters*, vol. 99, no. 12, Article ID 126802, 2007.

[5] A. Schiffrin, T. Paasch-Colberg, N. Karpowicz et al., "Optical-field-induced current in dielectrics," *Nature*, vol. 493, no. 7430, pp. 70–74, 2013.

[6] E. Bialic, L. Maret, and D. Kténas, "Specific innovative semi-transparent solar cell for indoor and outdoor LiFi applications," *Applied Optics*, vol. 54, no. 27, pp. 8062–8069, 2015.

[7] S. Lei, L. Ge, Z. Liu et al., "Synthesis and photoresponse of large GaSe atomic layers," *Nano Letters*, vol. 13, no. 6, pp. 2777–2781, 2013.

[8] A. F. Qasrawi, H. K. Khanfar, and R. R. N. Kmail, "Optical conduction in amorphous GaSe thin films," *Optik—International Journal for Light and Electron Optics*, vol. 127, no. 13, pp. 5193–5195, 2016.

[9] D. Olguín, A. Rubio-Ponce, and A. Cantarero, "Ab initio electronic band structure study of III–VI layered semiconductors," *The European Physical Journal B*, vol. 86, no. 8, article 350, 2013.

[10] O. Madelung, *Semiconductors: Data Handbook*, Springer Science & Business Media, New York, NY, USA, 2012.

[11] H. Fujiwara, *Spectroscopic Ellipsometry: Principles and Applications*, John Wiley & Sons, London, UK, 2007.

[12] D. K. Schroder, J. L. Benton, and P. Rai-Choudhury, *Diagnostic Techniques for Semiconductor Materials and Devices*, Electrochemical Society, Pennington, NJ, USA, 1994.

[13] G. R. Fowles, *Introduction to Modern Optics*, Dover, New York, NY, USA, 1989.

[14] A. R. Ward, T. O. Ward, and Z. McBride, "Hand held system for antifungal treatment," US 20130211481 A1, 2013.

[15] Y. Jin-Sung, L. Myung-Jae, P. Kang-Yeob, and C. Woo-Young, "10-Gb/s 850-nm CMOS OEIC receiver with a silicon avalanche photodetector," *IEEE Journal of Quantum Electronics*, vol. 48, no. 2, pp. 229–236, 2012.

[16] H. S. Nalwa, *Handbook of Advanced Electronic and Photonic Materials and Devices*, Academic Press, London, UK, 2000.

[17] V. N. Katerinchuk, Z. R. Kudrynskyi, and Z. D. Kovalyuk, "Spectral anisotropy of a photoresponse from heterojunctions based on GaSe and InSe layered crystals," *Technical Physics*, vol. 59, no. 3, pp. 407–410, 2014.

[18] S. Y. Sarkisov, A. V. Kosobutsky, V. N. Brudnyi, and Y. N. Zhuravlev, "Ab initio calculations of optical constants of GaSe and InSe layered crystals," *Physics of the Solid State*, vol. 57, no. 9, pp. 1735–1740, 2015.

[19] W. Y. Liang, "Optical anisotropy in GaSe," *Journal of Physics C: Solid State Physics*, vol. 8, no. 11, pp. 1763–1768, 1975.

[20] J. Lekner, *Theory of Reflection of Electromagnetic and Particle Waves: Of Electromagnetic and Particle Waves*, Springer, Hingham, Mass, USA, 1987.